

Damage zone propagation and support pressure estimation around two access tunnels of the Barapukuria coalmine in Bangladesh: a two-dimensional numerical modeling approach

Md. Rafiqul Islam ^{1*}, Mohammed Omar Faruque ¹, Ryuichi Shinjo ²

¹ Department of Petroleum & Mining Engineering, Shahjalal University of Science & Technology, Sylhet 3114, Bangladesh

² Department of Physics & Earth Sciences, University of the Ryukyus, Okinawa, 903-0213, Japan

*Corresponding author E-mail: dmrislam74@gmail.com

Abstract

The present study uses a two-dimensional boundary element method (BEM) numerical analysis to predict damage zone propagation associated with the required support pressure estimation around the two access tunnels of Barapukuria coalmine in northwest Bangladesh. Two tunnels at different depths are presented here. The stability of the two tunnels that was driven through the weak rocks' strata of Gondwana formation is examined at depths below the surface 290 m and 453 m. The two tunnels involve horseshoe-shaped design. The shallower tunnels, which are located below the surface 290 m, are presented by model A. The deeper tunnels, which are located below the surface 453 m, are presented by model B. Both tunnels are horseshoe-shaped with a height of about 4.5 m and 4 m, respectively. The modeling analysis was carried out in two stages to predict the damage zone and required support pressure. The first stage considered the model without support installation. The second stage measured the model with non-uniform internal support pressure installation. It is reasonable to mention that prior and subsequent to the support pressure estimation, three important parameters, like-strength factor, failure trajectories, and deformation boundaries in the vicinity of the two tunnels have been computed properly. Final results reveal that the strength factor values ranged from 0.33 to 0.99 would create the intense deformation at the roof and sidewalls. The damage zone would be extended from 0.64 to 0.74 m towards the roof and sidewalls. The damage zone would be ranged from 1.95 to 2.21 m, for shallower and deeper tunnels, respectively. For shallower tunnels, the required support pressure would be ranged from 4.0 to 9.0 MPa. For deeper tunnels, the essential support pressure would be ranged from 7.0 to 14 MPa.

Keywords: Boundary Element Method; Access Tunnel; Barapukuria Coalmine; Bangladesh.

1. Introduction

The natural state of stress within sub-surface rock mass is usually disturbed by an excavation. The presence of mines or metro tunnels disturbs the in-situ state of stress (Yavuz 2006). The excavation method, face supports pressure, excavation rate, stiffness of support system, and excavation sequence has dramatic effects on ground deformations that occur due to tunneling operations (Ocak 2009). Stress redistribution and deformation of the rock start occurring ahead of the opening face (Yavuz 2006, Islam et al. 2009, Islam & Shinjo 2009a, Islam & Shinjo 2009b). It is well known that the basic parameters affecting the ground deformations are related to the underground geological conditions and technical parameters of tunnel (Karakus & Fowell 2003, Tan & Ranjit 2003, Minguez et al. 2005, Ellis 2005, Suwansawat & Einstein 2006, Ocak 2009). Before the development of mine access tunnels, technical parameters include tunnel depth and geometry, tunnel diameter, single or double track lines, and neighboring geological structures. Construction method, which leads a safe and economic pro-

ject, should be planned so that ground movements will be limited to an acceptable level (Ocak 2009). Estimation of stress and deformation in the ground due to the excavation of tunnel (Bobet 2009) is a significant task for developing coalmines in Bangladesh (Fig.1). Prediction of stresses, deformations and damage zone propagation associated with the estimation of the support pressure at the surrounding grounds of the two access mine tunnels of coalmine is essential. Over the past several decades, perhaps the best-known analytical solution used for preliminary prediction of support measure is the boundary element method (BEM) numerical simulation. The main objective of the study is to estimate first, the propagation of the damage zone around two horseshoe-shaped tunnels, and then to predict the required strength of support system around two tunnels of the Barapukuria coalmine (Fig.2) in Bangladesh, which is the first coalmine of the country. The required support pressures were assessed by means of examine2D software package of rocsicene.com.

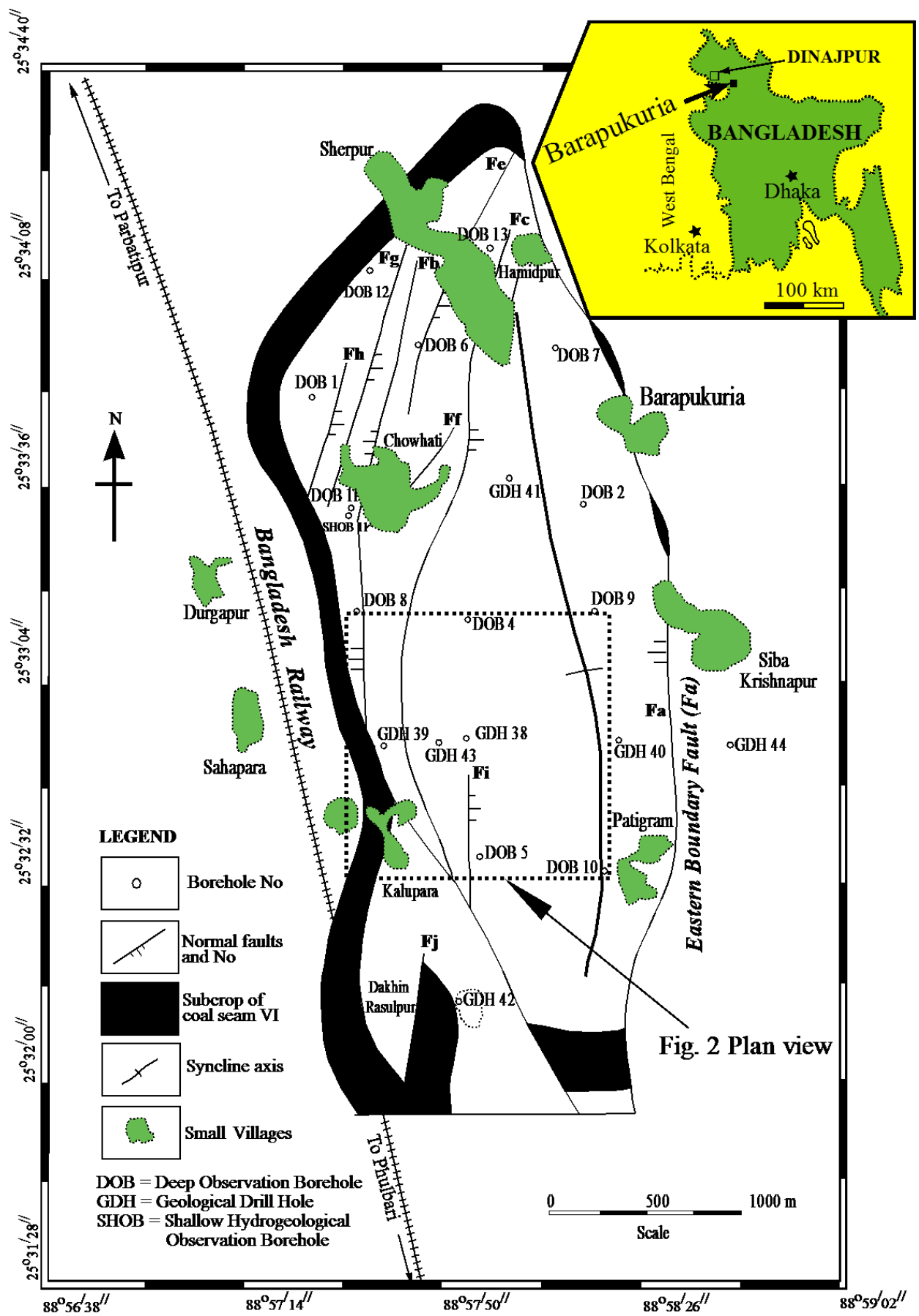


Fig. 1: Location of the Barapukuria Coal Mine, NW Bangladesh (Islam & Shinjo 2009a)

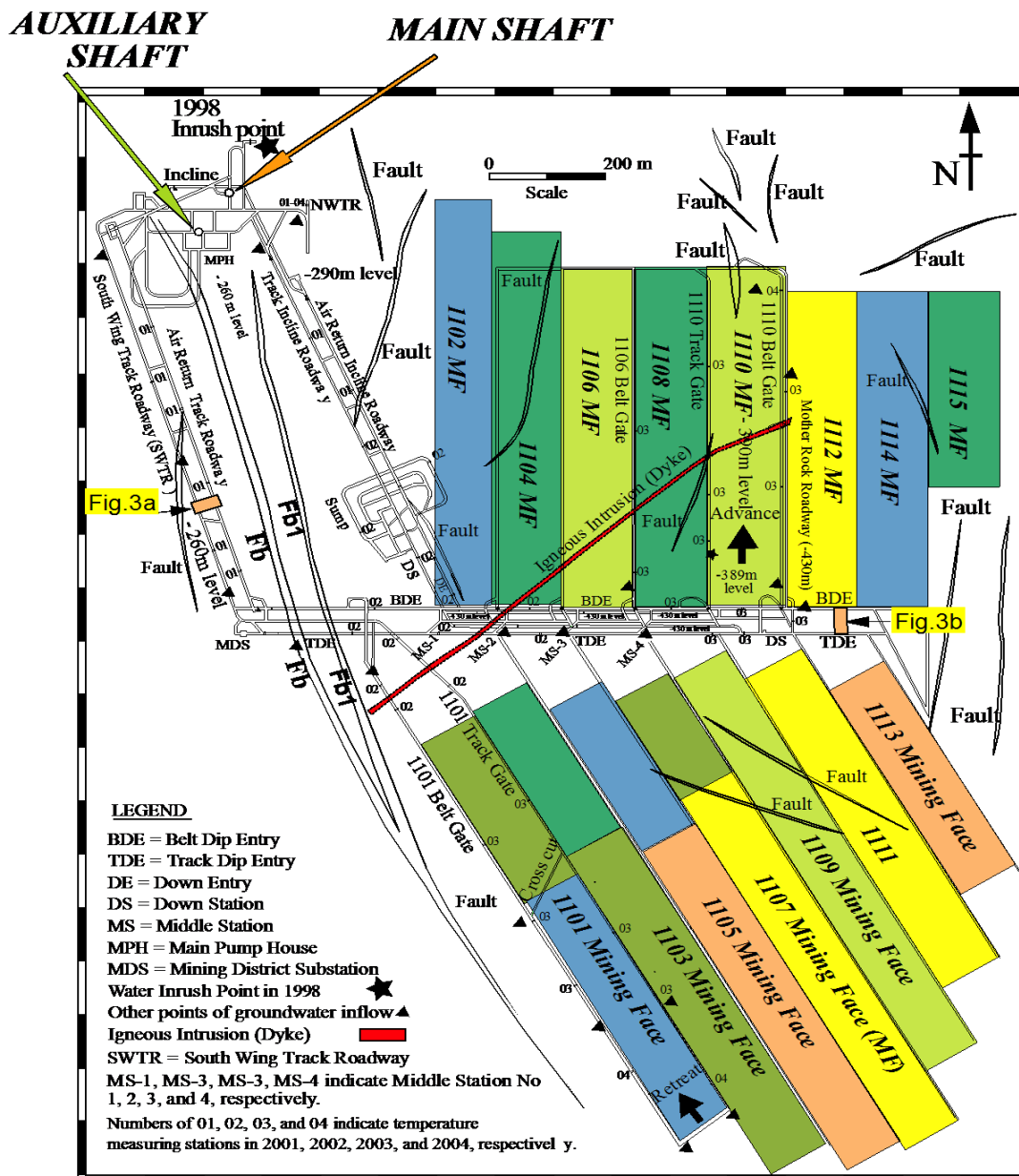


Fig. 2: Longwall Mining Panels in Barapukuria Coal Mine, Bangladesh (Islam & Shinjo 2009a).

2. Numerical modeling

Different numerical methods have been applied widely for modeling the underground excavations. The most familiar methods are finite element, finite difference, boundary element, discrete element and hybrid methods. The present study used boundary element method (BEM) numerical modeling. The term 'boundary element' is used to indicate the method whereby the external surface of a domain is divided into a series of elements over which the functions under consideration can vary in different ways, in such the same manner as in finite elements. In terms of mining engineering, the boundary of the underground excavation is divided into elements and the interior of the rock mass is represented mathematically as an infinite continuum (Islam & Shinjo 2009b). The present study emphasizes the role of excavation-induced stresses that lead to the damage zone propagation of the rock surrounding to the two access tunnels before support system installation. At first, we attempt to appraise the damage zone propagation around the two tunnels. Then the computation was carried out to detect the required strength of support system. We applied the software package Examine2D (www.rocscience.com).

2.1. Geometry and location of the two tunnels

Three different openings, like- circular, horseshoe and rectangular in shape, are commonly practiced in mining and civil engineering underground constructions (Yavuz 2006). In the Barapukuria underground coalmine, horseshoe-shaped tunnels were constructed for serving the extraction of ore reserves. The idealized excavation geometry and dimension of horseshoe-shaped openings for the models (A and B) are given in Figure 3ab. Figs. 2 and 3 represent the location and cross-sections of the two tunnels. The shallower tunnel, which is located beneath the ground surface of 290 m (model A), has a horseshoe shape with a height of 4.5 m and a width of 4 m (Fig.3a). The deeper tunnel, which is located beneath the ground surface of 453 m (model B), has also a horseshoe shape with a height and width of 4.5 m and 4 m (Fig.3b).

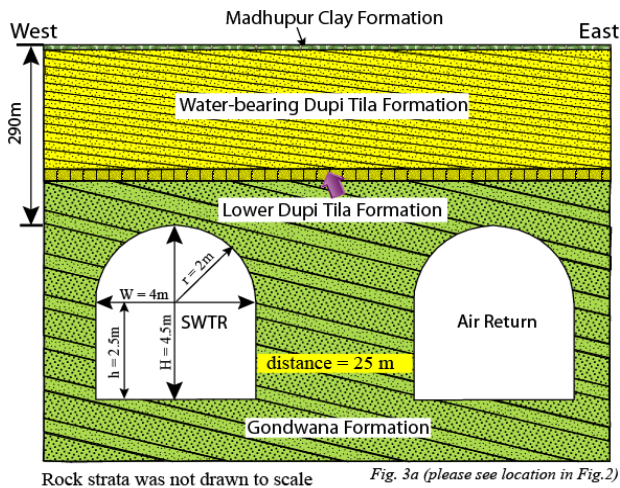
2.2. Geology around the two tunnels

The study area is located in the northwest part of Bangladesh. The geology and stratigraphy of the Gondwana Barapukuria coal deposit was illustrated in detail by [Islam & Hayashi 2008, Islam et al. 2009, Islam & Shinjo 2009a]. The geological formations mainly consist of sedimentary rocks. The geology of the study area consists of the following formations:

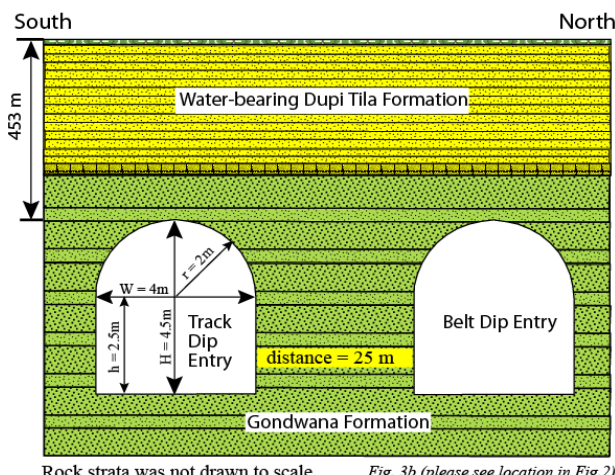
- Holocene-recent aged Madhupur Clay Formation, about 1-15 m thick,

- Late Miocene-Middle Pliocene aged water-bearing aquifer Dupi Tila Formation (DTF), about 100-220 m thick,
- Permian-aged coal-bearing Gondwana Formation, about 133-390 m thick ,and
- Pre-Cambrian Achaeen basement.

The main rock types along the tunnel alignment include sandstone, siltstone of the Gondwana formation, which is gray in color. Joint spacing ranges from 50 to 80 cm and is classified as widely spacing. Highly persistent joints are observed and 1 to 2 mm wide apertures are filled with silty sand. Lithology around the tunnels is shown in Fig. 3ab. During the construction period, no major joints were observed around the two tunnels. Some minor joints were filled by using probe drilling activities associated with injection grouting. Therefore, in the present numerical modeling, geological discontinuities, e. g., faults and joints were not considered.



Rock strata was not drawn to scale Fig. 3a (please see location in Fig.2)



Rock strata was not drawn to scale Fig. 3b (please see location in Fig.2)

Fig. 3: Sectional Views of Two Assess Tunnels (See Location in Fig.2) With A Depth of 290 M and 453 M. Both Tunnels were driven through Gondwana Group of Rock Strata That Mainly Consists of Sandstone and Siltstone with a Dip of About 15o to 21o from West to East.

2.3. Rock mechanical properties

Five rock mechanical parameters for the Gondwana Formation, including unit weight, Poisson's ratio, Young's modulus, cohesion, and angle of internal friction, used in the modeling are listed in Table 1 (Wardell Armstrong 1991).

Table 1: Imposed Rock Mechanical Properties (Wardell Armstrong, 1991)

	Type	Gravitational stress
Stress field	Ground surface elevation (m)	290 (model-A)
	Ground surface elevation (m)	453 (model-B)
	Overburden unit weight (MN/m ³)	0.024
Rock mass elastic properties	Type	Isotropic
	Young's modulus, E (MPa)	10000
	Poisson's ratio, ν	0.25
	Type of failure	Mohr-Coulomb
Rock mass strength	Tensile strength (MPa)	0.3
	cohesion, c (MPa)	0.75
	angle of internal friction, ϕ (deg.)	28

3. Modeling results

Results of the numerical simulation are illustrated in Figs. 4-9. The modeling results are presented in terms of five rock mechanical parameters:

- Distribution contours of mean stress,
- Distribution contours of differential stress,
- Distribution contours of maximum shear stress (τ_{max}),
- Distribution contours of total displacement, and
- Distribution contours of strength factor.

3.1. Model A

The distribution contours of mean stress, which is expressed by $(\sigma_1 + \sigma_3 + \sigma_2)/3$ in the two-dimensional modeling, from the simulation using model A are shown in Figs. 4ab. The mean stress contour was about 5.76 MPa at the immediate roof of the model A (Fig. 4a) and ultimately increased to 6.40 MPa toward the roof. The stress value was about 2.56 MPa at the immediate floor that increased gradually toward the interior of the strata. Mean stress, with values up to 7.04 MPa, was concentrated in the immediate rib sides (Fig. 4ab). The distribution contours of differential stresses, which are expressed by $(\sigma_1 - \sigma_3)$ (www.rocscience.com), of model A are shown in Figs. 5ab. Low differential stress values were concentrated in two places: the immediate roof and the floor. In the rib sides, these values decreased gradually toward the interior of the rock strata. In the immediate roof, the maximum calculated stress value was 8.20 MPa (Fig. 5a) and 7.50 MPa (Fig. 5b) that were eventually reduced to 4 MPa. In the floor, the maximum stress value was 6.10 MPa and was ultimately reduced to 4.70 MPa. The shear stress values ranged from 5.40 to 11.70 MPa at the rib sides (Figs.5ab). The maximum shear stress (τ_{max}) distribution contours of the model A is illustrated in Figs. 6ab. The shear stress ranged from 1.0 to 3.0 MPa and was concentrated in an area that extended to the left-hand side of the roof and the right-hand side of floor. The shear stress ranged from -0.9 to -2.9 MPa and was concentrated in an area that extended to the left-hand side of the floor and the right-hand side of the roof. Maximum total displacement value of 0.0025 m (Figs. 7ab) was simulated for both the immediate roof and floor. Displacement values decreased gradually toward the roof and the floor.

The failure trajectories and strength factor values within unsupported rock strata around the two shallow tunnels are illustrated in Figs. 8ab. The strength factor values ranged from 0.33 to 0.99 around the tunnels that ultimately increased to the interior part of the rock strata. The value of strength factor less than 1 and failure trajectories within the rock strata around tunnels indicate propagation of the damage zone. It is observed that the damage zone extends up to 0.64 m towards the immediate roof, 1.06 m at the right-hand side of the roof, and about 1.0 m at the left-hand side of the roof. The damage zone that occurred at the sidewalls calculated to be much higher than that on the roof. The extents of the maximum damage zone at the left and right sidewalls were about

1.95 m and 1.96 m, respectively (Figs. 8ab). Required support pressures to protect roof, floor and sidewalls are shown in Figs. 9ab. The initial support pressure applied to the deformation boundaries of the horseshoe opening was about 4.5 MPa at the sidewalls, 8.5 to 9.0 MPa at the opening was about 4.5 MPa at the sidewalls, 8.5 to 9.0 MPa at the immediate roof, and 4.0 to 6.0 MPa to the left and right hand sides of the immediate roof. After installation of initial support pressure, strength factor at the immediate roof and sidewalls was 1.31, and 1.64, respectively.

3.2. Model B

The distribution contours of mean stress with its magnitudes of model B are shown in Figs. 4cd. The mean stress value was about 9.1 MPa at the immediate roof that ultimately increased to 10.1 MPa toward the roof. The values ranged from 9.1 MPa to 13.1 MPa at the sidewalls of the two tunnels. The differential stress contours of model B are shown in Figs.5cd. High stress values were concentrated at the sidewalls, where the stress values ranged from 17.80 to 8.8 MPa, from sidewalls to interior of the rock strata, respectively. Low stress values were concentrated at the immediate roof. The calculated stress value was 11.80 MPa (Fig. 5c) that were eventually reduced to 5.80 MPa.

The distribution contours of shear stress (τ_{max}) value of the model B is illustrated in Figs. 6cd. The stress ranged from 1.4 to 5.2 MPa and was concentrated to the left hand side of the roof. The value ranged from 1.4 to 2.3 MPa to the right hand side of floor. The minimum shear stress value ranged from -1.5 to -5.3 MPa at the right hand side of the roof. The value ranged from -0.5 to -2.5 MPa at the left hand side of the floor. Total displacement value of 0.0040 m (Figs.7cd) was calculated at the immediate roof of the two tunnels. Displacement values decreased gradually toward the roof and sidewalls. The deformation vectors, strength factor, and failure trajectories are illustrated in Figs. 8cd. The strength factor values ranged from 0.33 to 0.99 around the tunnels that eventually increased to the interior part of the rock strata. The strength factor value less than 1 indicates damage zone within rock strata. The damage zone extends up to 0.74 m towards the immediate roof, 1.04 m at the right hand side of the roof, and about 1.05 m at the left hand side of the roof. The extent of damage zone was 2.19 m at the left sidewall and 2.21 m at the right sidewalls (Figs. 8cd). Essential support pressures in the vicinity of the two deep tunnels are shown in Figs.9cd. The required support pressure value ranged from 6.8 to 7 MPa at the sidewalls, 13 to 14 MPa at the immediate roof, and 7 to 11 MPa to the left and right hand sides of the immediate roof. After installation of initial support pressure, strength factor at the immediate roof and sidewalls was 1.31, and 1.64, respectively.

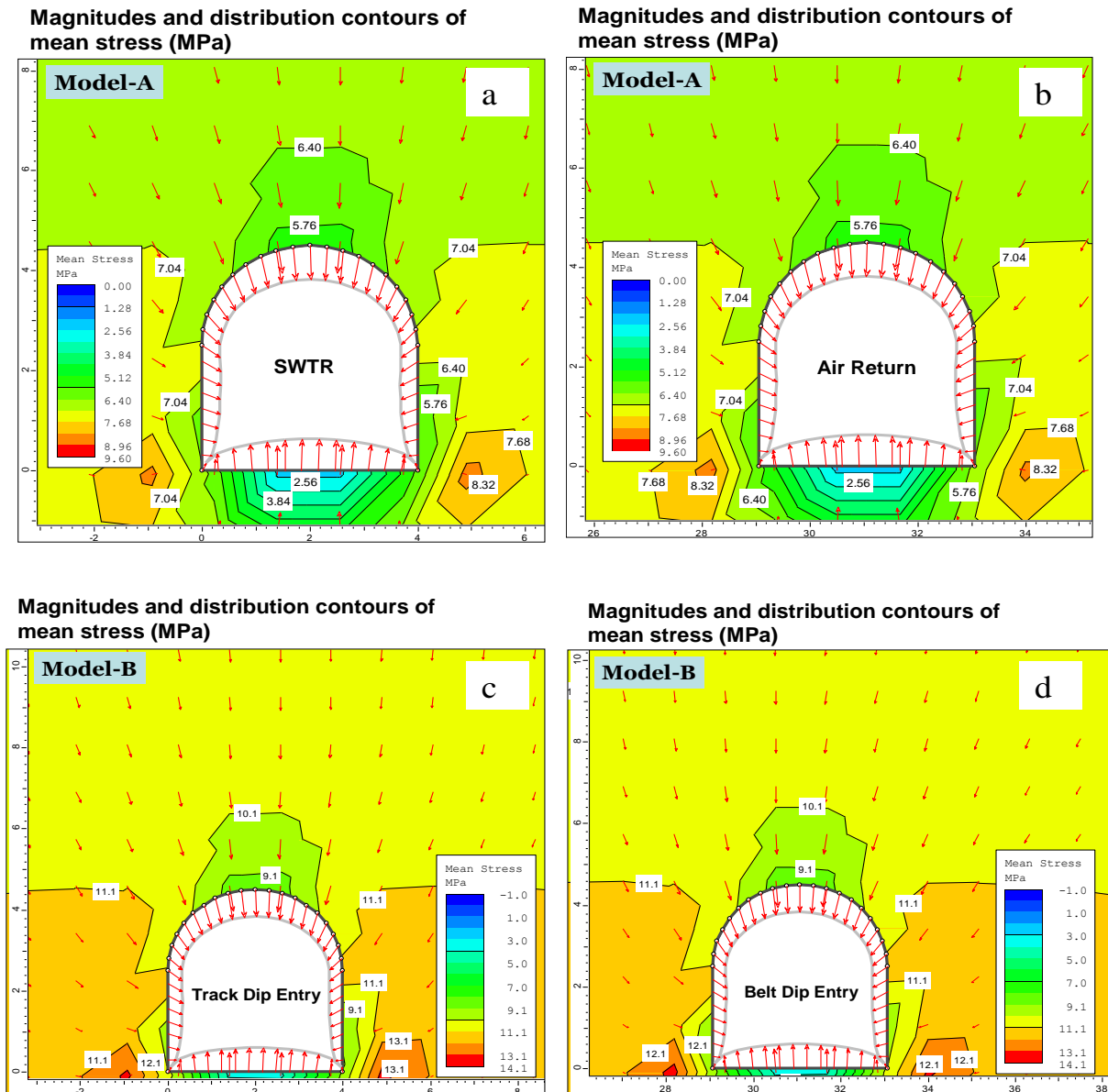
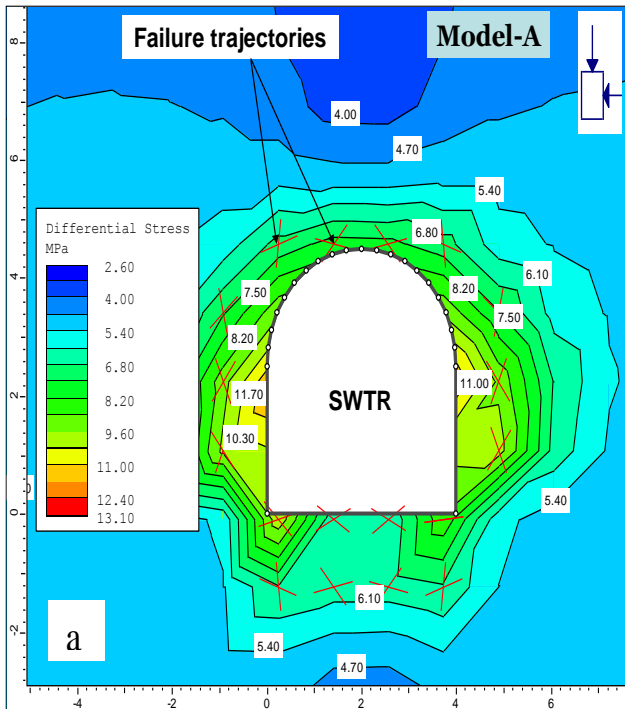
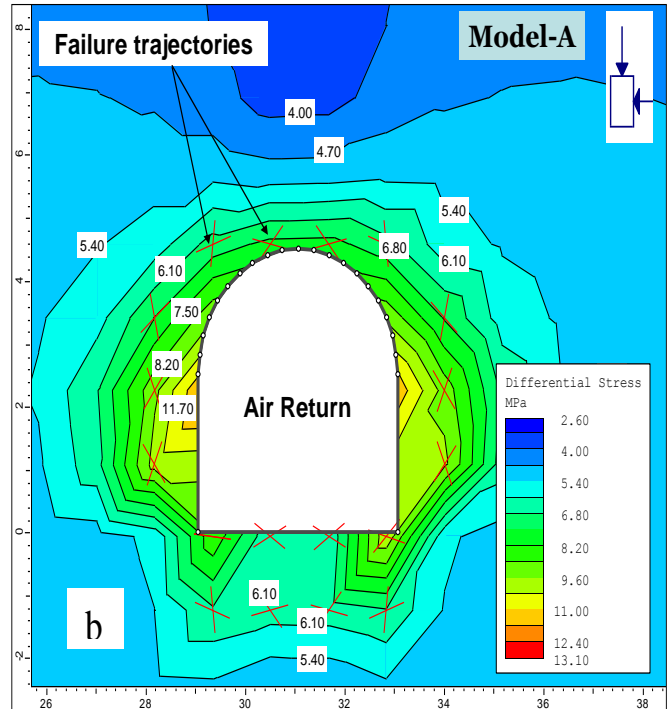


Fig. 4: (A-D) Magnitudes and distribution contours of mean stress (MPa)

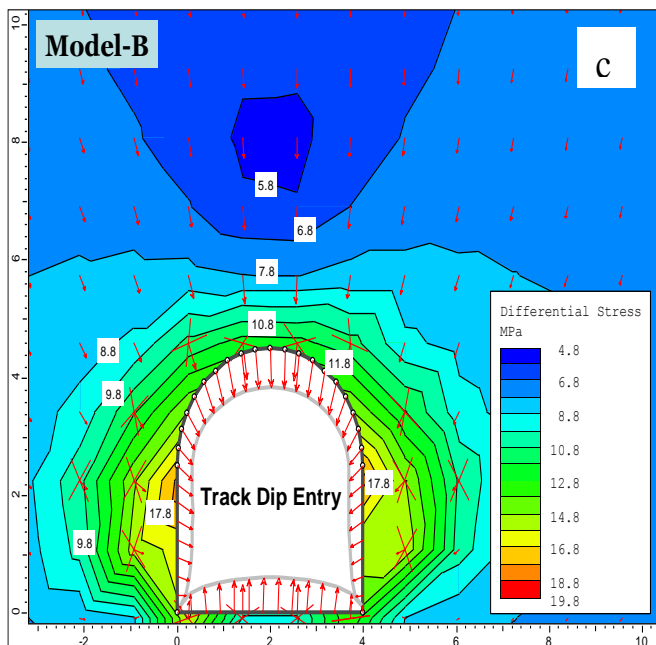
Magnitudes and distribution contours of differential stress (MPa)



Magnitudes and distribution contours of differential stress (MPa)



Magnitudes and distribution contours of differential stress



Magnitudes and distribution contours of differential stress

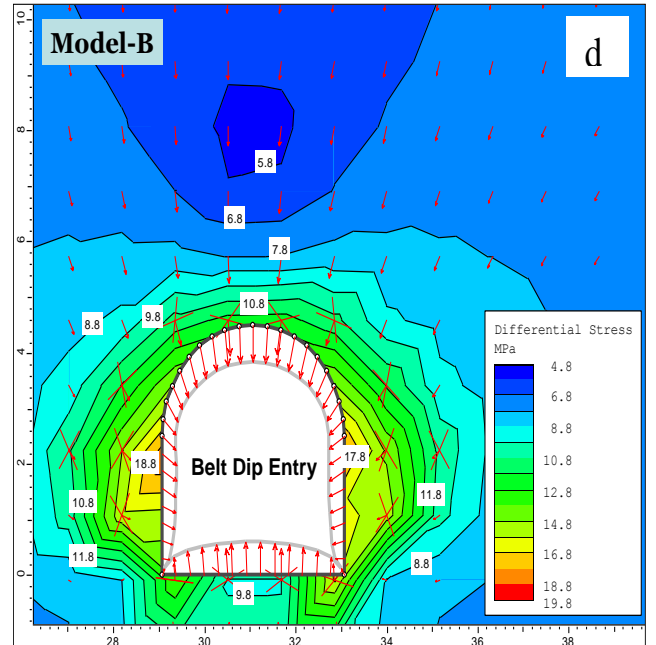
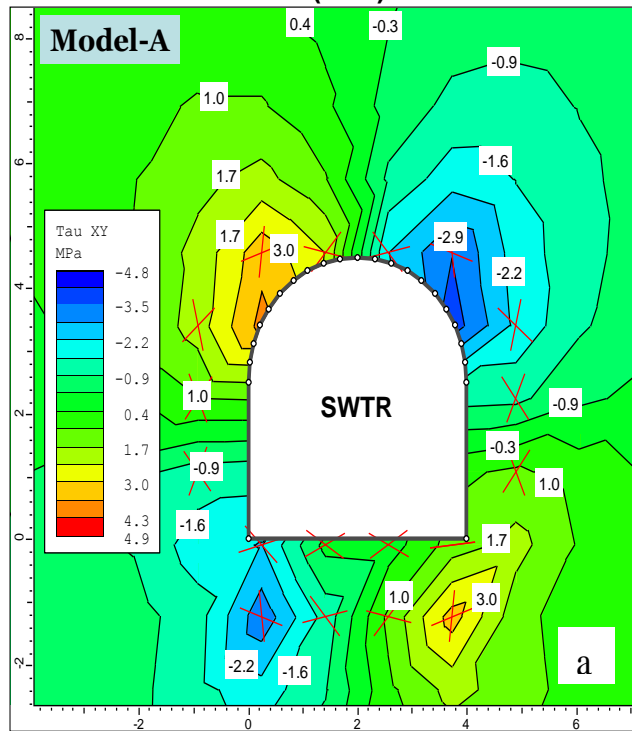
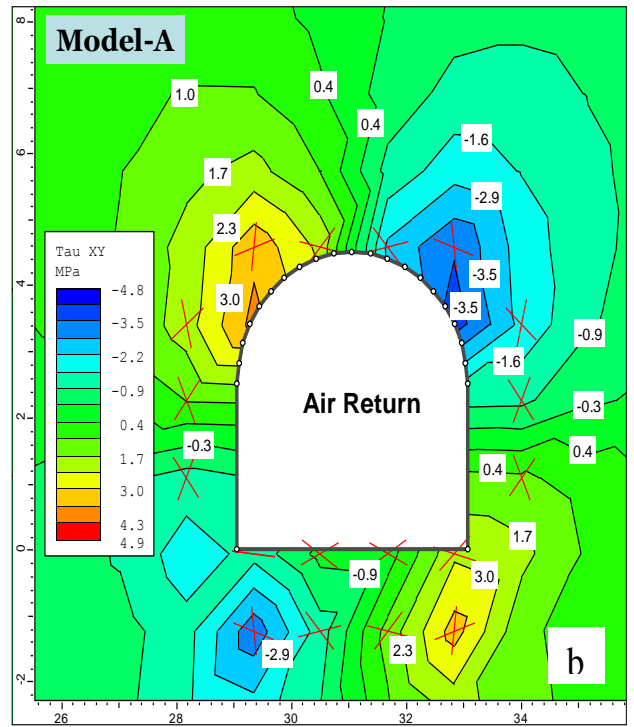


Fig. 5: (A-D) Magnitudes and Distribution Contours of Differential Stress (MPa)

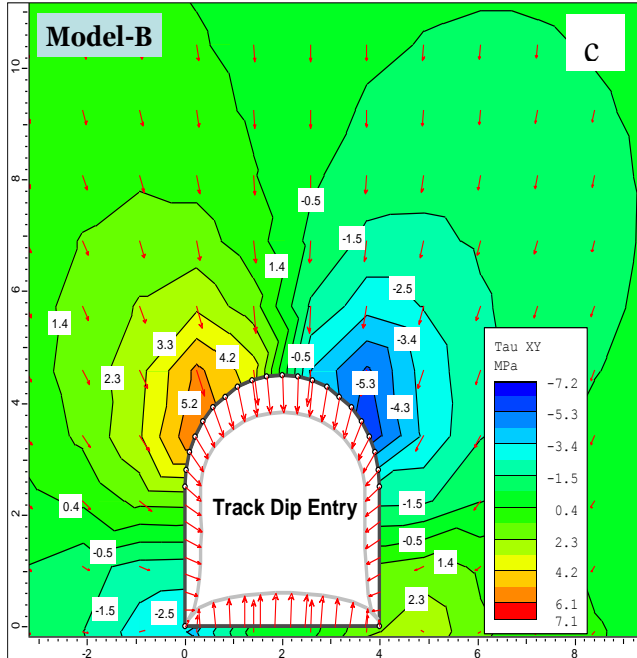
Magnitudes and distribution contours of maximum shear stress (MPa)



Magnitudes and distribution contours of maximum shear stress (MPa)



Magnitudes and distribution contours of maximum shear stress



Magnitudes and distribution contours of maximum shear stress

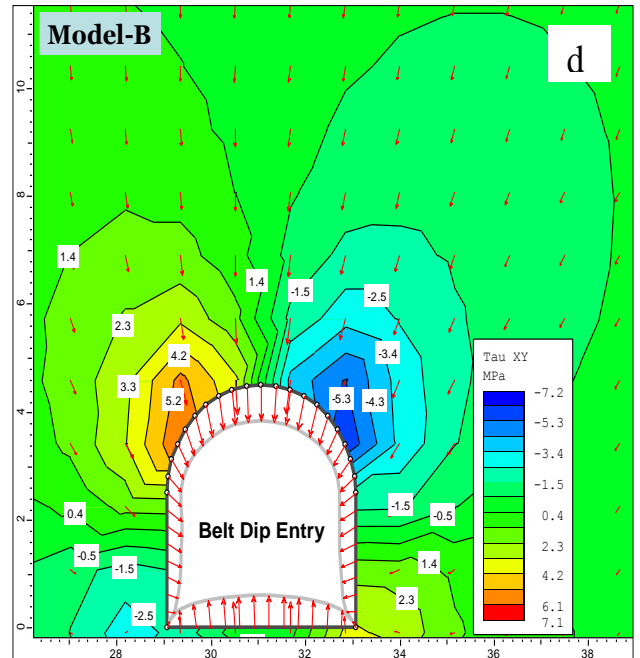
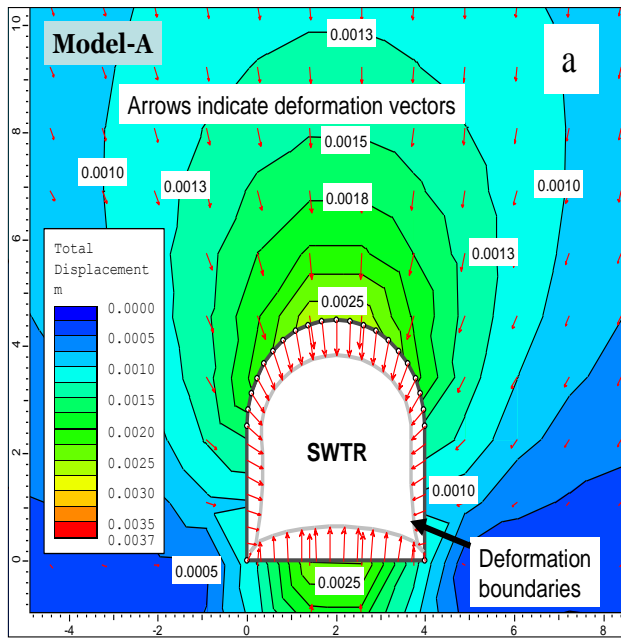
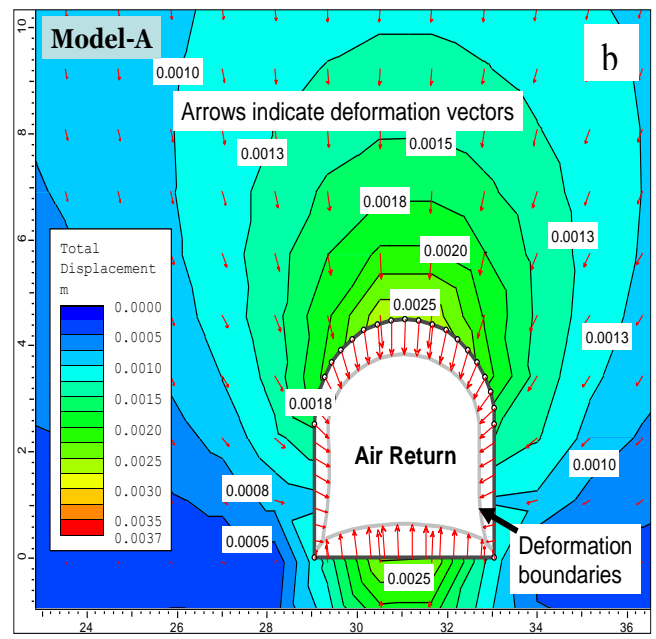


Fig. 6: (A-D) Magnitudes and distribution contours of maximum shear stress (MPa)

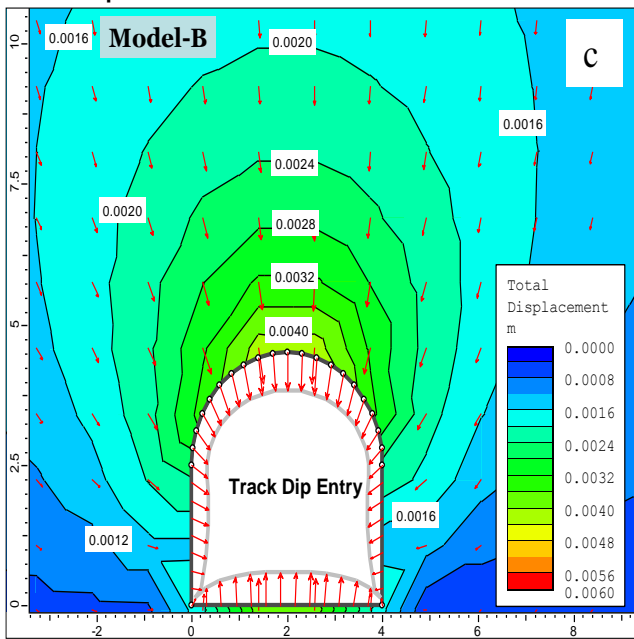
Magnitudes and distribution contours of total displacement (m)



Magnitudes and distribution contours of total displacement (m)



Magnitudes and distribution contours of total displacement



Magnitudes and distribution contours of total displacement

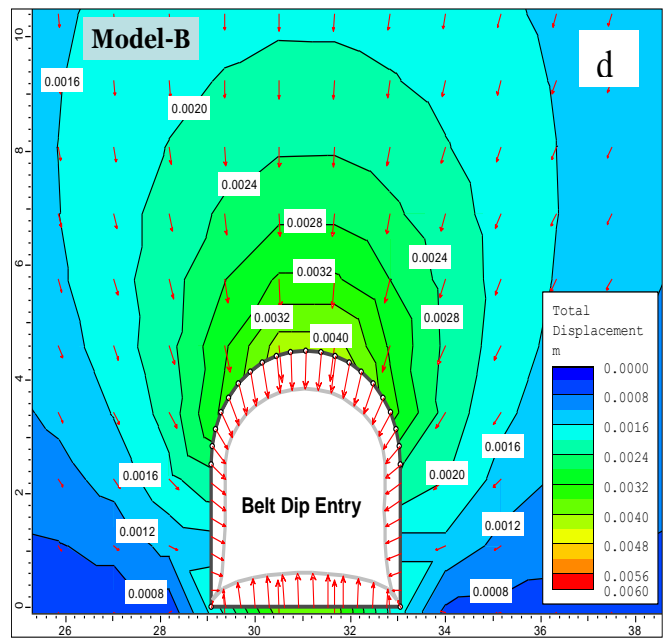
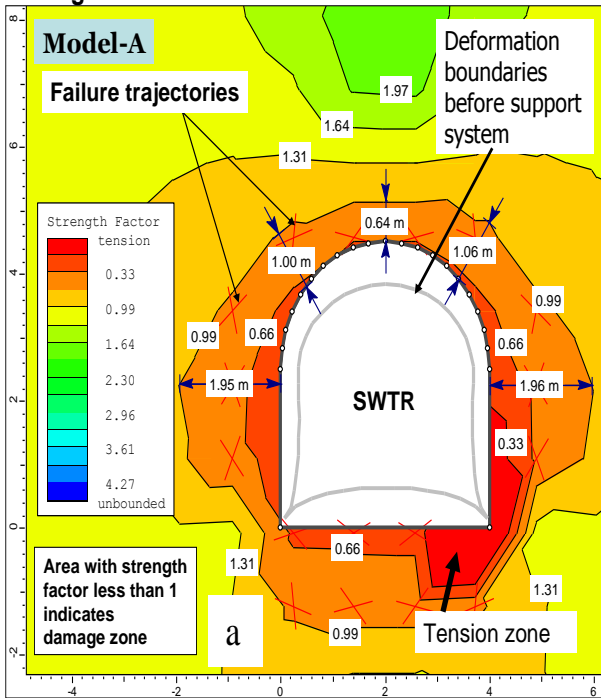
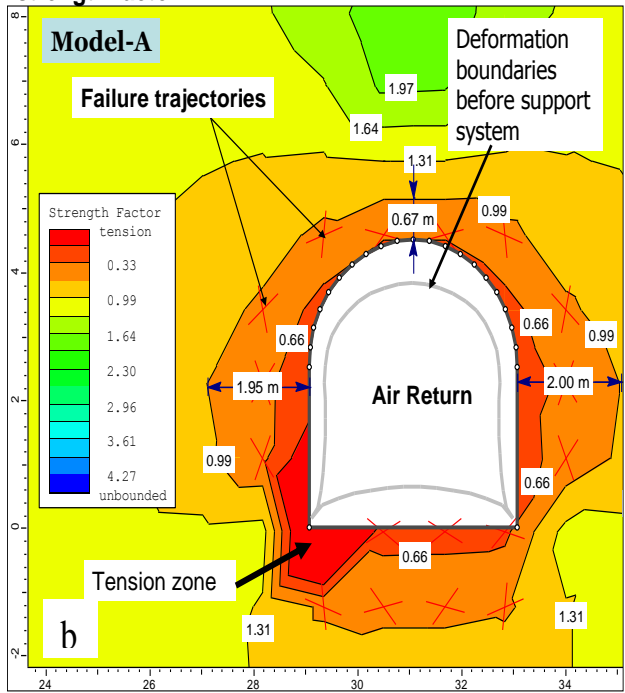


Fig. 7: (A-D) Magnitudes and Distribution Contours of Total Displacement (M)

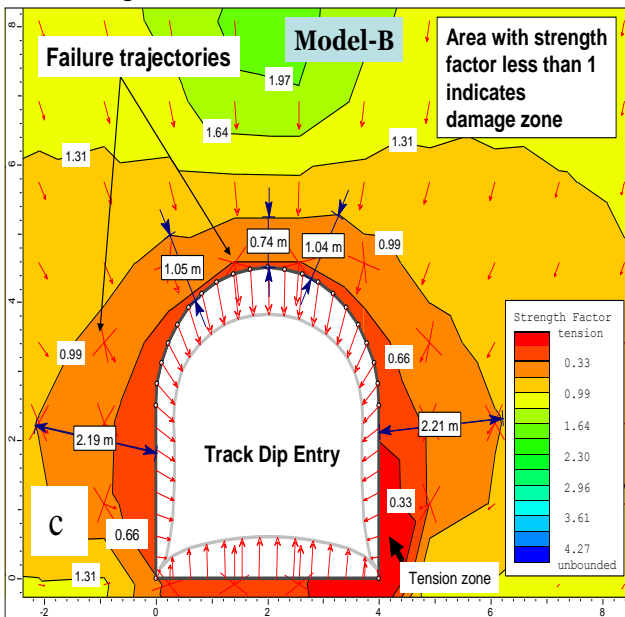
Magnitudes and distribution contours of strength factor



Magnitudes and distribution contours of strength factor



Magnitudes and distribution contours of rock strength factor



Magnitudes and distribution contours of rock strength factor

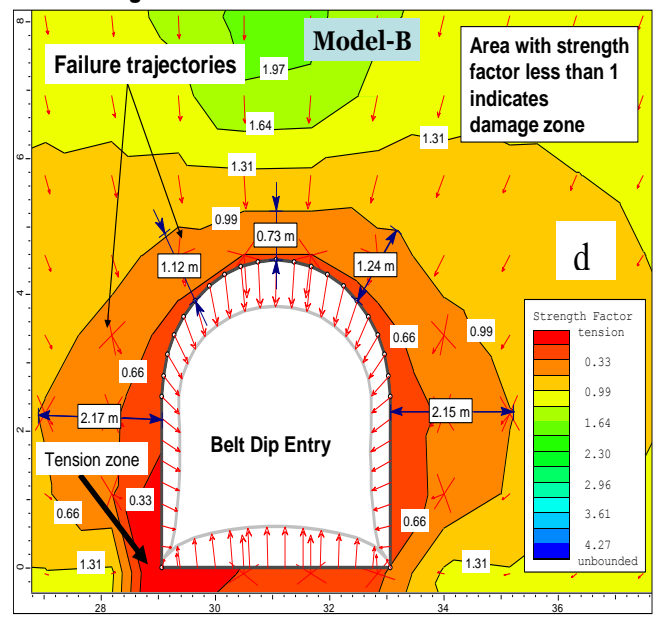


Fig. 8: (A-D) Magnitudes and distribution contours of strength factor

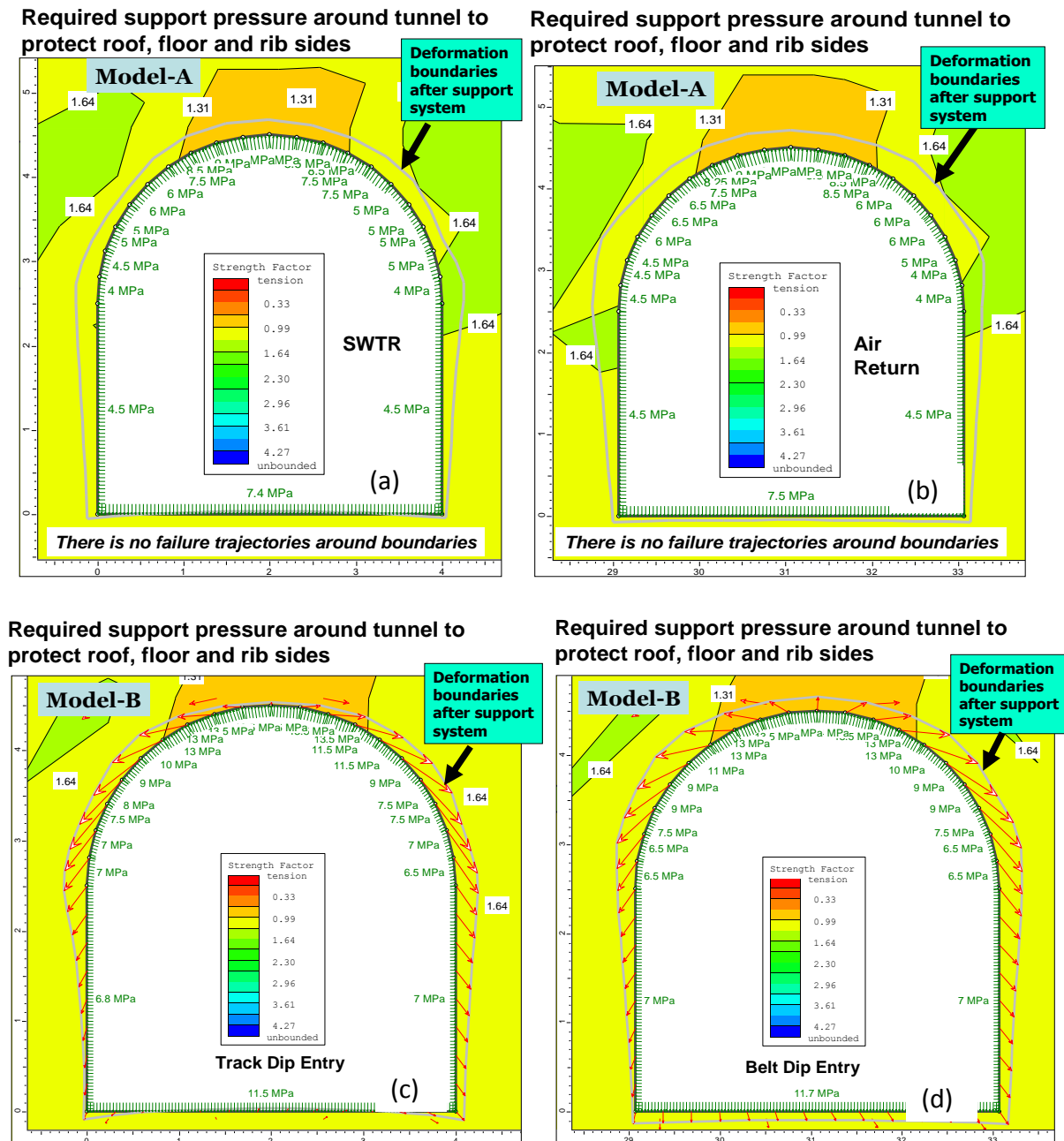


Fig. 9: (A-D): Required Support Pressure around Tunnel to Protect Roof, Floor and Rib Sides

4. Discussions and conclusions

In weak rocks mass, for example, the Barapukuria coalmine area (Islam & Hayashi 2008, Islam & Shinjo 2009a, Islam & Shinjo 2009b), the stability of tunnels usually involves instability of the face as well as failure in the rock mass surrounding the tunnel (Hoek 1998). In the present study, damage zone and support pressure design of the two access tunnels of the Barapukuria coalmine in Bangladesh is considered by the use of numerical analysis. The two access tunnels involve a 4 m span horseshoe-shaped design driven through weak rocks of the Gondwana formation. The stability of the two tunnels is examined at depths below surface 290 and 453 m. Deformation of the underground opening, like underground mining tunnels, depends mainly on the properties of rock mass, stress state; dimensions shape of the opening, time effect and support system effect (Yavuz 2006, Hoek 1998). In the present numerical modeling, three important parameters- for example, (i) strength factor, (ii) deformation trajectories, and (iii) deformation boundaries in the vicinity of the two access tunnels have significantly been focused under the in situ stress field.

In order to simulate the two-dimensional effects of the tunnels' advance, the analysis was carried out in two stages. In the first stage, the model, without the support installed (Figs. 8a-d), was allowed. To consolidate under the in situ stress field. In the second stage, the tunnels were considered with non-uniform internal support pressure (Figs. 9a-d) that was applied to the internal boundary of the tunnels. For the case of two-dimensional numerical modeling, all three principal stresses (σ_1 , σ_3 and σ_2) are used in the calculation of the strength factor. If the strength factor is greater than 1, this indicates that the material strength is greater than the induced stress. If the strength factor is less than 1, this indicates that the stress in the material exceeds the material strength (i.e. the material would fail). If the strength factor contours indicate tension, this means that σ_3 is less than the calculated negative stress (tension) cutoff for the Mohr-Coulomb failure criterion (www.rocsience.com) (Islam & Faruque 2012). The failure trajectories within the rock strata around the tunnels indicate propagation of damage zone. The damage zone within surrounding strata would be spread over to rock strength factor less than 1.

The magnitudes and distribution of the strength factor value ranged from 0.33 to 0.99 in the present numerical models (A and B) specify that the intense deformation of the roof strata would extend from 0.64 to 0.74 m towards the roof. The extent of the damage zone and displacements along the boundary of the horse-shoe opening cross-section caused a non-uniform extent of the damage zone. The maximum damage zone at the sidewalls ranged from 1.95 to 2.21 m for shallow and deep tunnels, respectively. The damage zone that occurred at the sidewalls calculated to be much higher than that on the roof.

Required support pressures for the both tunnels are shown in Figs.9a-d. For the case of model A, the required support pressure would be about 4.5 MPa at the sidewalls, 8.5 to 9.0 MPa at the immediate roof, and 4.0 to 6.0 MPa to the both sides of the immediate roof. For the case of model B, the essential support pressure in the vicinity of the two deep tunnels would be ranged from 6.8 to 7.0 MPa at the sidewalls, 13 to 14 MPa at the immediate roof, and 7 to 11 MPa to the both sides of the immediate roof. After installation of the required support pressure (Figs.9a-d), the deformation boundaries in both models (A and B) were replaced to the outside of the original shape of the tunnels. Applied support pressure enhanced the strength factor of rock strata that increased to 1.31 at the immediate roof and 1.64 at the sidewalls. It is reasonable to focus that concrete lining associated with strength of about 7.4 MPa, and 11.7 MPa are required to protect floor heave of model A, and Model B, respectively.

References

- [1] Bobet, A., 2009. Elastic Solution for Deep Tunnels. Application to Excavation Damage Zone and Rockbolt Support. *Rock Mechanics and Rock Engineering* 42(2), 147–174. <http://dx.doi.org/10.1007/s00603-007-0140-0>.
- [2] Ellis, D., 2005. High standards in Heatrow's art. *Tunnels and Tunneling International* 37(9), 29–34.
- [3] Hoek, E., 1998. Tunnel support in weak rock. Proc. Reg. Keynote address, Symposium of Sedimentary Rock Engineering, Taipei, Taiwan, November 20-22, pp.1–12.
- [4] Islam, M. R and Hayashi, D., 2008. Geology and coal bed methane resource potential of the Gondwana Barapukuria Coal Basin, Dinajpur, Bangladesh. *International Journal of Coal Geology* 75, 127–143. <http://dx.doi.org/10.1016/j.coal.2008.05.008>.
- [5] Islam, M.R., Hayashi, D., Kamruzzaman, A.B.M., 2009. Finite element modeling of stress distributions and problems for multi-slice longwall mining in Bangladesh, with special reference to the Barapukuria coal mine. *International Journal of Coal Geology* 78(2), 91–109. <http://dx.doi.org/10.1016/j.coal.2008.10.006>.
- [6] Islam, M.R., and Shinjo, R., 2009a. Mining-induced fault reactivation associated with the main conveyor belt roadway and safety of the Barapukuria Coal Mine in Bangladesh: Constraints from BEM simulations. *International Journal of Coal Geology* 79(4), 115-130. <http://dx.doi.org/10.1016/j.coal.2009.06.007>.
- [7] Islam, M.R., and Shinjo, R., 2009b. Numerical simulation of stress distributions and displacements around an entry roadway with igneous intrusion and potential sources of seam gas emission of the Barapukuria coal mine, NW Bangladesh. *International Journal of Coal Geology* 78(4), 249 –262. <http://dx.doi.org/10.1016/j.coal.2009.03.001>.
- [8] Islam, M.R., and Faruque, M.O., 2012. Numerical modeling of slope stability consideration of an open-pit coalmine in the Phulbari coal basin, NW Bangladesh. *Electronic Journal of Geotechnical Engineering (EJGE)* 17(y): 3717-3729.
- [9] Karakus, M., Fowell, R.J., 2003. Effects of different tunnel face advance excavation on the settlement by FEM. *Tunneling and Underground Space Technology* 18(5), 513–523. [http://dx.doi.org/10.1016/S0886-7798\(03\)00068-3](http://dx.doi.org/10.1016/S0886-7798(03)00068-3).
- [10] Minguez, F., Gregory, A., Guglielmetti, V., 2005. Best practice in EPB management, *Tunnels and Tunneling International* 37, 21–25.
- [11] Ocak, I., 2009. Environmental effects of tunnel excavation in soft and shallow ground with EPBM: the case of Istanbul. *Environmental Earth Sciences* 59(2), 347–352. <http://dx.doi.org/10.1007/s12665-009-0032-6>.
- [12] Suwansawat, S., Einstein, H. H., 2006. Artificial neural networks for predicting the maximum surface settlement caused by EPB shield tunneling. *Tunneling and Underground Space Technology* 21(2), 133–150. <http://dx.doi.org/10.1016/j.tust.2005.06.007>.
- [13] Tan, W.L., Ranjit, P.G., 2003. Parameters and considerations in soft ground tunneling, *Electronics Journal of Geotechnical Engineering* 8(D), ppr0344_3.
- [14] Wardell Armstrong, 1991, *Techno-Economic Feasibility Study of Barapukuria Coal Project* (unpubl.), Dinajpur, Bangladesh.
- [15] Yavuz, H., 2006. Support pressure estimation for circular and non-circular openings based on a parametric numerical modelling study. *The journal of the South African Institute of Mining and Metallurgy* 106(2), 129-138.